978-1-5090-0903-9/16/$31.00 ©2016 IEEE

Object Stability during Human Precision Fingertip Manipulation

Yuri Gloumakov, Thomas Feix, *Member IEEE*, Ian M. Bullock, *Student Member IEEE*, and Aaron M. Dollar, *Senior Member, IEEE*

Abstract— **Fingertip-based manipulation is one of the hallmarks of human hand function. However, there are clear limitations to the stability of these grasps, whether it is due to digit lengths or the friction between the object and the finger pad. The present work focuses on the stability of point-contact grasps during rotational movements of objects 50 mm and 80 mm in diameter over the range of the workspace. The mean angle achieved during all the trials for each digit ranged from 2° to 76°, with the thumb generally having larger mean angles. During the trials the object would often lose contact with individual digits, and we suspect that it is due to the angle that the object made with each of the digits. Object size had little significance predicting this angle, while the number of digits used, which digit, and axis of rotation were significant. Angles 0.125 s and 0.025 s prior to loss of contact between digit and object were regarded as unstable. Unstable angles in the negative elevation direction (angles that are often achieved when the digit is extended) occurred in 64% of the trials and in the positive elevation direction in 23% of the trials. In 57% of the trials unstable angles lied in the positive azimuthal direction and in 29% of the trials lied in the negative azimuthal direction. The four fingers, disregarding the thumb, were found to have very similar instability regions when manipulating the object about the X-axis (ulnar-radial) and the Y-axis (distal-proximal), where most of the trials, 72%, have had the majority of their unstable angles occurring in the negative elevation direction and 62% occurring in the positive azimuthal direction.**

I. Introduction

Human within-hand manipulation capabilities are in a large part what separates our superior dexterity from even our closest primate relatives. However, in order to achieve a substantive range of motion, contacts with the object being manipulated must be minimal, as each contact adds constraints to the mobility. The tradeoff to fewer contacts for increased manipulability is therefore a decrease in the force closure capabilities, and therefore object stability. In this study, we experimentally examine the stability of precision fingertip grasps during object manipulation about the three rotational axes (distal-proximal, ulnar-radial, and palmar-dorsal) (Figure 1). We tested subjects' tendency to lose contact with grasped objects at various points on the edge of the manipulation workspace as a function of number of fingers used and two different object sizes.

We hope that this study will expand upon our understanding of the limitations and capabilities of the human hand and be able to help provide benchmarks and inspiration for robotic and prosthetic hand design [1]–[4]. Rehabilitation for paretic hands of stroke and hemiplegic cerebral palsy patients could greatly profit from a richer understanding of hand function during manipulation tasks. Knowing how to design haptic interfaces, such as those used in surgical robotics [5], will improve overall performance [6]. Furthermore, our results could shed light on the redundancy of fingers when handling these devices and which configurations are preferable.

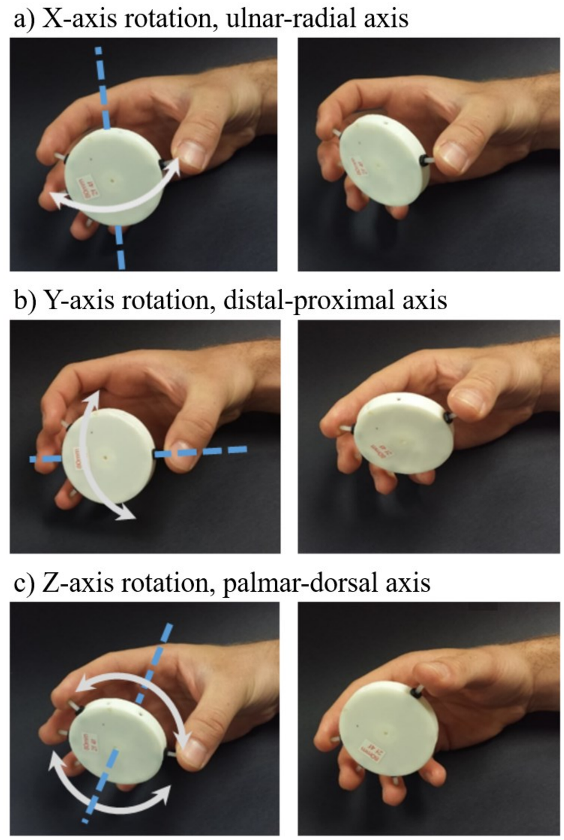

Figure 1. Demonstration of manipulation movements for one of the objects (80 mm) used in this study.

Past research on grasp stability in robotic and human hands has taught us a lot about successful static and dynamic grasps. Certain groups have focused on tactile data [7] and probabilistic models for stability assessment in robotics [8]. Other work focused on robotic hands undergoing blind grasping, i.e. without sensory feedback at all, by simulating all possible postures using a grasp database [9]. Human hand grasping has been studied with respect to the neurological control of the finger forces when picking up objects with various friction coefficients [10]. Although manipulation of objects has been studied to some extent [11], the stability of dynamic in-hand object manipulation is still a young field.

This work was supported in part by the National Science Foundation grants IIS-1317976 and IIS-0953856.

Y. Gloumakov, T. Feix, I. M. Bullock, and A. M. Dollar are with Yale University, New Haven, CT 06511 USA, (email: {yuri.gloumakov, thomas.feix, ian.bullock, aaron.dollar}@yale.edu).

Prior work by the authors has focused on translational [12] and rotational [13] workspaces of in-hand manipulation , as well as using a similar fingertip usage analysis to identify regions of the fingertips that were most commonly used [14]. However, stability of grasps were not investigated in depth. Other studies have shown that individuals regulate finger contact forces to minimize overall force and maintain stable grasps [11] and add more fingers to increase the hands' ability to resist forces and grasp larger objects [15], [16]. Fingers apply different amounts of normal and shear forces, and yet the limits of the in-hand workspaces are not fully understood. This study hopes to gain insight into the mechanisms underlying workspace limitation as well as the ability of each digits to maintain contact with the object that lend themselves to achieve fewer drops or repositions and greater grasp stability.

II. MATERIALS AND METHODS

Subjects manipulated different sized objects while varying the number of digits used. The sensorized objects were rotated back and forth in order to explore the limitations of the rotational range around a particular axis and angles that the object made with the finger pad were recorded. The study was approved by the local Institutional Review Board.

A. Participants

17 healthy, unimpaired, right handed subjects were recruited to participate in our experiment. They were reached either through flyers or by personal communication. Most participants were affiliated with the university. Ten subjects were male and seven female. Left-handers were deliberately excluded and only the dominant right hand was used in this study so as to simplify the experimental set up as well as to record the maximum dexterous motion of each participant. The mean hand length was 18.1 cm (males: 18.47 cm, females: 17.5 cm) and the mean age was 26.9 years (range: 21-41 years). Hand lengths were measured from the tip of the middle finger to the base of the palm using a 12" ruler. Digit thicknesses were measured using calipers.

B. Equipment

A trackSTAR magnetic tracking system (Ascension Technologies, Burlington, VT) with a medium range transmitter and eight Model 180 2 mm diameter sensors were used to record the motions at 80 Hz. Five sensors were taped to the back of the finger nails of the user's right hand, one sensor was placed into the center of the object (and replaced into other objects throughout the experiment), and two sensors were placed on the back of the user's right hand to act as a local reference point with which the 6-D rotation and location information of the other sensors were calculated. Since the global position of the hand was not changed, all the rotational and translational motion was evoked by digit motion only. Sensors placed on the hand were secured using Vapon Topstick® and Top Stick® Men's Grooming Tape.

There were 4 objects in total where each object had the capacity for two different finger configurations; the objects with 4 pins allowed for 2 and 4 digit trials, while the objects with 5 pins allowed for 3 and 5 digit trials. For the trials that required a lower number of digits, the outermost pins were not used. The objects had pins of about 2.6 mm in diameter, and were spaced out at about 40º radially as inspired by a study which found a consistent angular pattern for finger placement [17].

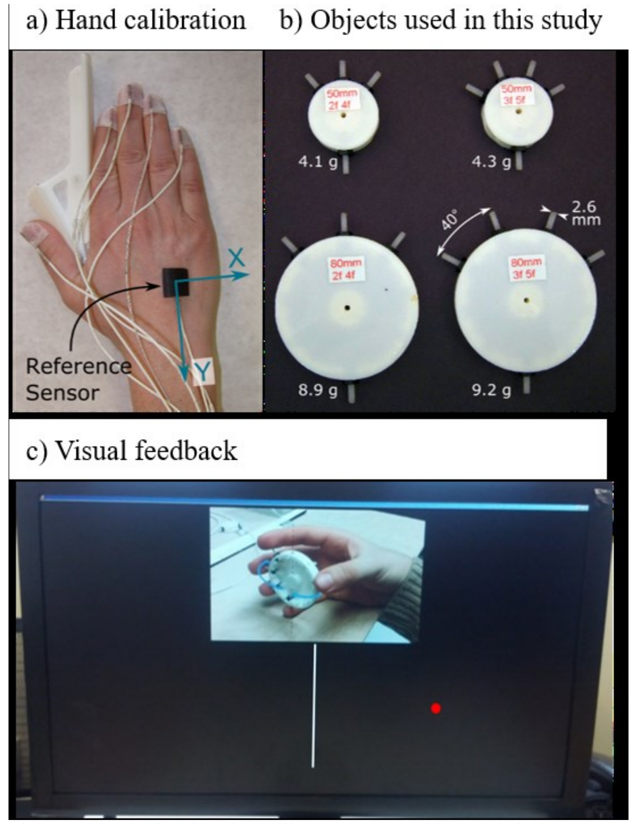

Figure 2. a) The hand in the calibration setup. This step is important as it defines the rotational axes. b) The four objects used in this study and their properties. The small objects have a diameter of 50mm (including the screw lengths), whereas the large object is 80 mm. c) The image at the top half of the screen was present throughout the trial to indicate the required motion. The vertical white line sat at the calibrated zero mark, while the red dot ran horizontally indicating the current rotation progress around the required axis. Other rotations had no affect on the feedback.

Visual feedback was presented using a 27" LCD monitor placed about 1 m in front of the subjects above the table (Figure 2). Subjects were able to observe their rotation progress throughout the experiment. The screen was also used to indicate the required motion for the trial.

C. Procedure

Participants were first introduced to the experiment and the types of digit motions that they will be required to make through a brief presentation using various videos depicting the correct "back-and-forth" rotation motion around each of the three axes. In total there were 48 30-second trials (each trial was executed twice): 2 (thumb and index), 3 (thumb, index, and middle), 4 (thumb, index, middle, and ring), or 5 digits were used to rotate a 50 mm or 80 mm (in diameter) object, weighing about 4.2 g and 9.0 g respectively, through one of the three major axes. The object axes were regarded the same as the hand axes: distal-proximal (X-axis), ulnar-radial (Y-axis), and palmar-dorsal (Z-axis). Rotational movement, as opposed to translational movement, was chosen as it is much more likely to result in unstable grasp conditions, observed informally from previous work in the area [12], [13], experiments which focused on the in-hand

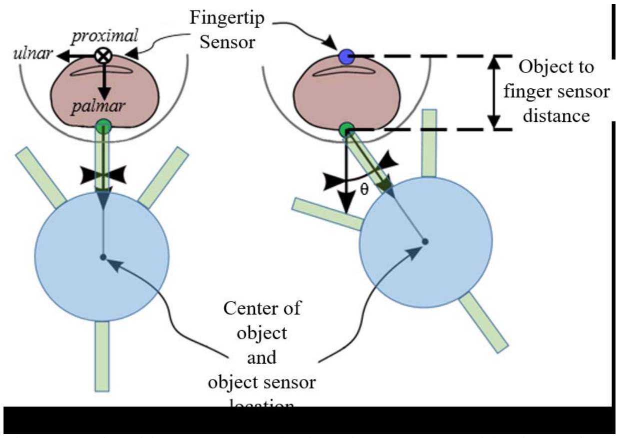

Figure 3. The object creates a single point contact, and it pivots about this point during the trials. The angles between the object and the finger pad normal were recorded, as seen in the image on the right. Object to finger sensor distance was used to define the initial finger thickness as well as detect any loss of contact. Using this image as an example, the angle above would lie in the negative azimuthal direction.

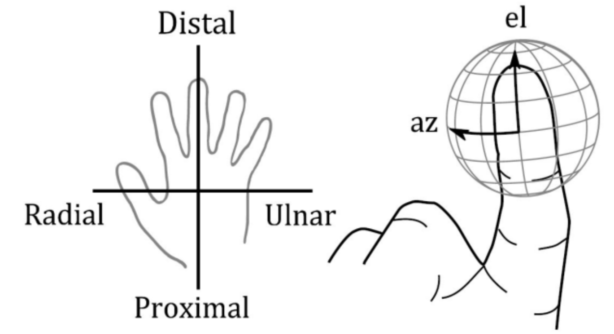

Figure 4. Major anatomical axes of the right hand are shown in the left image while the right image describes the spherical coordinates that are later used in the analysis. Dorsal-palmar axis is normal to the page. Elevation (el) is considered as the positive direction when the object is tilted towards the distal portion of the fingertip while the azimuth (az) is positive when the object is tilted towards the ulnar direction.

workspace. Each subject was instructed to place their hand into a specially constructed support and the object was placed in its tray for calibration (Figure 2). The object sensor was replaced and a new calibration took place every time a trial required the use of a different object. During the trials participants rotated the object from one extreme to the other in a comfortable cyclical motion. By limiting the rotations to one axis at a time, subjects were expected to achieve a larger range and come closer to the limits of their grasp stability. Prior to each trial, participants also had the chance to practice rotating the object while observing the object's rotation angles on the screen.

D. Fingertip Usage Analysis

Angles that the object made with each digit were calculated with respect to the finger pad. This was done by first translating the coordinates of the object sensor to the tip of the pin to locate the point of contact. Then using the dot product relationship we calculated the angle between two vectors that originate at the point of contact; one points toward the object sensor and the other pointing away from the finger sensor (Figure 3). By examining which angles led to drops and repositions of the objects during the trials, we can better understand which configurations are least stable. Thus, we devised a method that was capable of detecting a loss of contact between each digit and the object.

Determining when an object was "dropped" is difficult due to the compliance in the finger pads and the error in the sensor modality. We therefore utilize a threshold method that tracked the distance between the object and the digit sensor. The threshold was calculated as the distance between the digit sensor and the end of the object's pin (typically on the order of 5 mm), and it flagged the data points when that distance was deemed too great to maintain contact. The initial distance was found by averaging the first 40 frames (0.5 s) for every trial. 0.5 s was considered to be appropriate as we did not want to include the distances of any potential early drops or repositions that may have occurred. A threshold distance was selected based on a percent increase of the initial distance. Candidate thresholds were calculated by increasing from 100% in 5% increments until the number of object drops indicated by the algorithm was approximately the same as those visually recorded during the experiment. This threshold was then kept at the same percent increase for all of the trials, but due to the unique initial distances, the threshold distance varied from trial to trial. The threshold method predicted a "drop" when at most one digit was detected to maintain contact at a single moment. If a loss of contact was detected but at least two digits maintained contact with the object, then that trial was considered to have had a "reposition." A trial may only be labelled as either having a drop, reposition, or neither, since the criteria to detect a drop also satisfies the criteria that detects a reposition.

To create a visual representation of the angles, we had to project the three dimensional motion onto the surface of a sphere. In order to preserve the visual density of the points on a scatter plot, the Lambert azimuthal equal-area projection was used as recommended in [18]. For specifying positions on the sphere, elevation and azimuth angles are used [19], which are analogous to the latitude and longitude angles respectively that we see on geographical maps (Figure 4). The elevation and azimuth angles are mapped to spherical coordinates by

$$\theta = 90 - el, \ \phi = -az. \qquad (1)$$

By assuming that each point on the sphere is defined to have unit mass, we are able to find the center of the point cloud on the sphere by normalizing a simple Cartesian vector sum, which corresponds to the center of mass of the points. Because it is a spherical projection, some inevitable shape distortion will be present (Figure 5).

With these projections, it is difficult to see the spatial density (dispersion) of the data points, instead we mostly highlight the spread. The dispersion can be modelled in a few ways, such as using the elliptical Kent distribution or the rotationally symmetric Fisher distribution [14]. However, the values from these models are not intuitive and they do not relate back to more conventional statistical approaches. Instead, we will use a distribution-free approach by symmetrically expanding a cone with its axis at the mean orientation of the data until it encompasses 68% of the data points. The angles for these cones can then be interpreted similarly to a one standard deviation range of the point

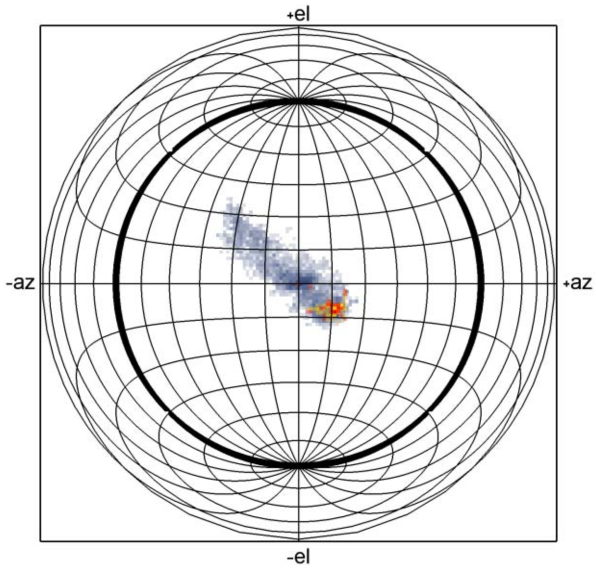

Figure 5. This single trial describes the workspace achieved by an index finger while a 50 mm object was rotated around the X-axis (distal-proximal) using 3 digits. The achieved angles are centered around the mean, highlighting the distribution as main focus. The red angles indicate the 2 points (0.025 s) and the orange angles indicate the 10 points (0.125 s) prior to loss of contact. Each line is separated by 15°. Note: multiple loss of contacts have occurred during this trial, hence we observe many orange and red points.

dispersion. While there are multiple possible cones that could contain a given percentage of the points, there is only one unique cone that can contain that percentage when centered at the mean of the points. This cone then projects onto the Lambert azimuthal equal-area projection as a second circle centered on the plot (aside from the one indicating the 180 degree circle).

Using the determined threshold, angles during which the digit has been considered to lose contact with the object were disregarded from the rest of the analysis, since once the contact was lost, recorded angles are essentially meaningless. Instead, angles two frames (0.025 s) prior to the loss of contact were colored in red. Angles ten frames (0.125 s) prior to the loss of contact were colored in orange. Only ten frames prior to loss of contact were labelled as it was the minimum length of time that it took for participants to rotate the object from one extreme to the other [13]. Note that only 8 frames were actually labelled as orange (frames 3-10 prior to loss of contact) since frames 1-2 prior to loss of contact were labelled red. Including both colors in the plots provided two essential descriptions of instability. First, it showed which specific angles were least stable. Second, it provided information regarding the direction in which the object was rotating prior to having lost contact with the digit by observing the relationship between the red and orange angles. A series of plots were then created that provide more generalized information regarding which angles resulted in the most loss of contacts. Trials were first centered on their mean so as to preserve the overall distribution, and to accommodate the different angle offsets that occur when the object was grasped at slightly different points of contact. This assumes that the point of contact itself does not affect the distribution in any major way, and the direction of instability was conserved.

For each individual trial we took the means and standard deviations of the angle data for all of the frames in a trial, angles that we called "red", and angles that we called "orange". In order to assess the difference in the angular shifts between these distributions we conducted a two-tailed t-test in both the azimuth and elevation directions separately, comparing the distribution of all angles with the orange and red angles in order to. In addition to identifying whether these distributions were significantly different from one another, we were also able to eliminate those factors in the trials were not significant in affecting the angular shifts. This was done using a multi-factor anova; the four trial conditions were the independent variables, while the angular shift of the unstable region was the dependent variable. Since we used a multi-factor anova, the order in which we tested the variables affected their significance. In order to avoid eliminating potentially important variables we ran the anova multiple times, each time changing the order of the variables. We only considered the lowest p-value, which is achieved when a variable is first in the order. Although the angular shift is a continuous variable, by using the two-tailed t-test as mentioned, we were able to categorize each trial and provide some interesting statistics regarding the propensity for the red and orange angles to be located in a particular quadrant. Angles recorded during the periods of loss of contact were not considered in these calculations.

III. Results

The rotation experiment was completed by 17 subjects with 792 trials overall. The first two subjects did not perform the 2 digit trials, however they were not excluded since the rest of the experimental protocol was the same. Trials in which the sensors were poorly calibrated and resulted in impossible angles between the object and the normal were ignored, thus out of the maximum 792 trials only 711 were considered. For a given type of trial (same number of fingers, axis, and object size) the mean angle achieved across all subjects is summarized for each digit (Table 1). A standard deviation was calculated for each trial type describing the

Table 1. Mean of all angles in degrees achieved during the different trials, excluding the angles recorded during loss of contact. Standard deviation for all trials is approximately 10º.

Axis of rotation		**X**		**Y**		**Z**	
Size (mm)		***50***	***80***	***50***	***80***	***50***	***80***
Thumb	***2***	20	11	19	17	39	31
	3	15	13	18	16	31	32
	4	26	22	35	26	37	30
	5	32	19	32	24	36	31
Index	***2***	61	60	64	60	52	57
	3	65	71	62	77	69	72
	4	64	66	63	62	68	76
	5	61	58	58	60	72	73
Middle	***3***	49	53	52	54	44	45
	4	53	54	46	54	45	59
	5	50	62	47	63	47	64
Ring	***4***	32	33	25	34	27	45
	5	41	52	36	48	37	49
Pinky	***5***	6	8	10	15	2	2
Number of fingers		**Mean angle (°)**					

spread of the angles around the mean (the offset), and was found to be approximately 10º for each trial.

A threshold distance of 170% of the nominal distance between the digit sensor and object tip (on the order of 8mm) was determined to give the best match to the manually-recorded incidences of drops. Using this threshold for loss of contact, the full results are shown in Figure 6, where trials with a drop (where only one or no fingers maintain a contact within the threshold region) are indicated in the dark bars, and trials with a reposition (where at least one finger loses contact but at least two contacts remain) are shown in light grey. The calculated two finger trials lack any reposition data since the algorithm does not account for any assisted repositions from using the other hand, and considers any loss of contact as the object being dropped.

Since there are many factors and relationships that could be focused on, it was essential to omit those factors that were not found to be important. The factors of interest were initially the axis of rotation, how many digits were used, the size of the object, and whether there was a difference between each the digits. The means of the distributions of all the angles and the unstable angles (the orange and red angles) in a trial were generally different in both the azimuth and the elevation directions. Using the anova analysis, we examined whether the influence of each of the trial conditions on the unstable angles was significant (**Error! Reference source not found.**).

Table 2. Multi-factor anova conducted on the angular shift of the unstable angles with respect to the overal angle distirbution for each of the trials. The lowest p-value of each variable is presented, as achieved by placing each variable first in the order when running the anova analysis. Note, digit refers to testing whether angular shifts depend on which digit we analyze. Significance was considered when the p-value is below 0.05.

P-VALUES	Orange angles		Red angles	
	Az	El	Az	El
# of digits used	0.06	0.03	0.13	0.04
Digit	3.9e-7	0.03	2.1e-7	0.09
Axis of rotation	2.1e-04	1.2e-07	6.1e-04	7.4e-12
Size of object	0.54	0.58	0.62	0.64

Since the digit, number of digits, and the axis of rotation factors exhibited significant predictive power in at least one of the tests, these variables were kept in the analysis, and in the consideration of our results. By omitting size from further analysis, we were able to summarize the spherical plots more densely by overlaying trials with different sized objects.

Prior to plotting the trials on the spherical projection, the data was first centered on its mean to accommodate angle shifts due to different grasping postures and points of contact (Figure 5). After centering, all of the trials were then stacked according to each digit, around which axis the object was rotated about, and how many fingers were used in the trial (Figure 7). This creates a summary of all trials that allow for a visual inspection of the unstable regions for each digit. As previously defined, unstable regions are defined as either the orange region (angles recorded 3-10 frames prior to loss of contact) or the red region (angles recorded 1-2 frames prior to loss of contact). Out of 711 trials, 567 plots that have been generated have had a loss of contact. Using a two-tailed t-test

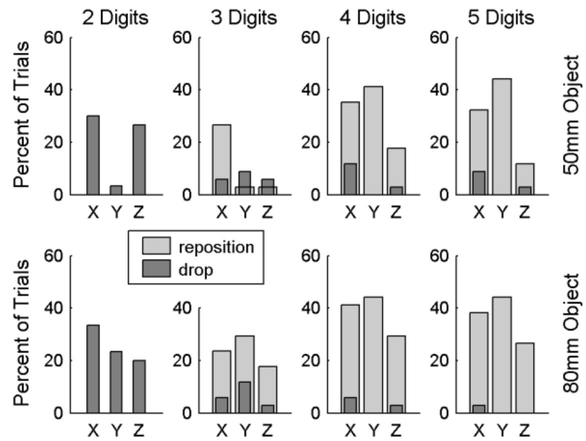

Figure 6. The predicted drops and repositions according to the estimated threshold. The trials that had a drop occur, were no longer considered to have a reposition due to overlapping labelling criteria.

in the azimuth and elevation directions for both the red and orange angles, we were able to summarize a few key points about these plots. Using the notation “[+el, -el, +az, -az]”, each element represents the percent of the plots that had their unstable angles significantly shifted towards that half. Out of 567 plots the angular shifts were as follows: [23, 64, 57, 29] for the orange angles and [17, 57, 49, 21] for the red angles. When considering slightly more specific cases, such as when the thumb is disregarded, out of 451 plots we saw the following: [22, 65, 61, 24] for the orange angles and [16, 58, 52, 18] for the red angles. When the Z-axis trials were subsequently disregarded, out of 343 plots we observed the following: [15, 72, 62, 23] for the orange angles and [11, 66, 53, 15] for the red angles.

IV. Discussion

Overall, the results show important aspects of the limitations of our grasps and posture instabilities, which can be used as inspiration for the design of prosthetics and robotic manipulators that can better predict and handle grasp success.

The mean angles for all the trials generally describe the posture with which the object was held. Due to the size of the object and/or the morphology of the hand, it may be impossible to hold the object with all digits normal to the pins. The median was not presented, as it was about the same as the mean and did not provide any new information. Likewise the standard deviation was omitted for each case as it was approximately the same across all conditions. What can be readily examined is that the angles with which the fingers made with the object are generally conserved no matter how many digits are used during the trial. It can also be observed that the average angle generally increases with larger object for the four fingers and decreases for the thumb. This is likely due to the natural posture of the hand when handling objects of various shapes that lend themselves to more stable grasps. The index finger exhibited the most extreme angle deviation, which could be due to its inability to directly face the center of the object. This suggests that the index in particular has a preferred direction that is not the center of a symmetric object in which it would be best at maintaining good contact. On the other hand, the pinky was

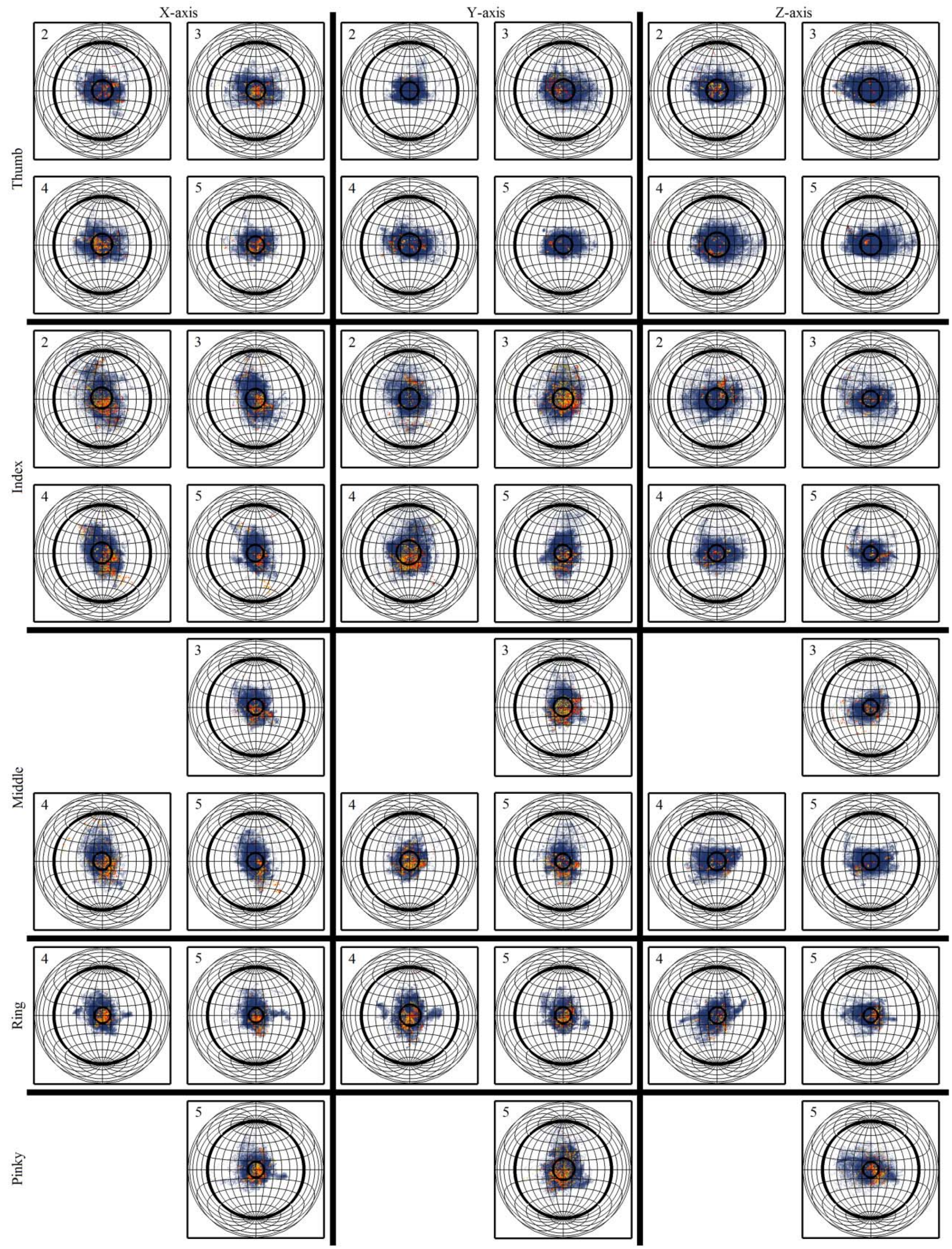

Figure 7. The aggregate of all the plots are presented according to each digit, around which axis the object was rotated, and how many fingers were used in the trial as indicated by the number in the corner of each plot. The numbers in the corner of each plot indicates how many digits were used. An equal-area projection is used to preserve apparent density of points. Shape distortion is fairly minimal for the data plotted. The blue points describe all the angles that were achieved by the participants. The orange points correspond to the angles within 0.125 seconds prior to the detection of the loss of contact. The red points correspond to 0.025 seconds prior to the detection of the loss of contact. The angles during which the object has been considered to lose contact with the digit are not displayed. The smaller bold circle in the center is the cone containing 68% of the points.

best at directly facing the object's center, and had very little deviation from the norm throughout the trials.

In order to understand the capacity of the human hand in maintaining grasp stability during point contact with objects, it is not enough to simply observe the mean angles, it is necessary to understand during which angles the subjects repositioned or dropped the objects. This type of analysis requires the precise timing of when the object was first found to have lost contact with the digits. For that we turned to creating a loss of contact model which identified the frames during which the sensor was deemed to have been too far from the object for it have maintained contact. Since the digit sensor was located on the nail of the digit, we had to estimate the digit thickness in order to locate the point of contact. To do that we took the average distance of the first 40 frames (0.5 s) of each trial between the digit sensor and the object's pin. We considered this to be a more accurate representation of the finger thickness than using calipers. This was due in part to the compliance of the finger pads, and when measuring with the calipers the experimenters could have been too generous with how much force to apply, whereas the model is more objective. It was also preferable to the calipers as it generated a new thickness prior to every trial as a way to compensate for slightly different grasp locations. And finally, the subjects themselves have applied different pressures on the object during the trials, thus effectively changing their digit thicknesses.

When deciding on a threshold as a percentage of the initial thickness, it was important to match the modeled drops and repositions to the observed drops and repositions as close as possible. A threshold too small causes a type a-error and too many trials would be falsely labeled as drops and repositions, and a threshold too great causes a type b-error and too few trials would be labeled as drops and repositions. The model performed very well when detecting drops, as was visually observed, with drops decreasing with added fingers. The amount of repositions that were observed generally decreased with added fingers, however, as can be seen in Figure 6 that was not the case for the model. This is to some extent an expected result, as the addition of fingers leads to an increase in the chance that one of them will lose contact with the object and be recorded as a reposition by the model, but left undetected by the experimenters. Greater number of digits also led to an increase in the chance of calculation error. However, this calculation is objective when looking for repositions. For example, the experimenters were often unable to detect when the subject momentarily lifted a finger while the model is not as forgiving. Finally, during the trials, certain digits were obstructed and observation of a reposition would have been impossible. Because of these reasons, we assumed the model to be an appropriate, if not more precise, estimation of loss of contact detection and the threshold.

By plotting each trial as an equal-area projection, we are able to better visualize the general shape of the rotational workspace, and by coloring the ten points prior to loss of contact and the two points prior to the loss of contact, we can see the regions of lower stability as well the direction in which the subjects tended to lose contact. The reason behind the choice to overlay the red over the orange angles, and both over the blue, is because it would better show how the object slips and its directionality, with the orange angles describing the motion that initiates the instability and the red assisting in the visualization of the direction of the motion. This can be effectively seen in Figure 5, where the red angles are further southeast than the orange angles. Angles prior to the loss of contact are a more reliable indicator of instability than the angles during the loss of contact, since a lack of contact between the object and the digits does not provide any useful angle data. The point of contact that the object made with the finger pad across all trials has been observed to range quite greatly, and thus in order to generalize the results, we centered all of the trials about their respective means, thereby focusing on the distribution of the angles achieved during the trials as well as the bias towards which quadrant in the az-el plots the losses of contact occurred.

Size of the object did not have a significant effect on the location of the unstable region and hence was excluded from further analysis. This led to a more condense description of the data. By visual inspection, we can get a sense of the trend of the unstable region, as well as the density of the plots by observing the size of the uncertainty cone, which contains 68% of the data. For example, despite the what can be readily seen in the final plot is the expected decrease in loss of contact of individual digits as the number of digits used increases, suggesting that added digits improves stability. This seems to be in contrast to the repositions that were detected by the model, but it is consistent since the aggregate losses of contact increases with added digits.

What has been surmised from the aggregate data is that unstable region tends to be biased to a particular direction in the equal-area projection plot. If we assume that the four fingers, excluding the thumb, behave in similar ways, then it would be predicted that they exhibit very similar loss-of-contact characteristics during the rotations around the X-axis, where they either move in the same direction simultaneously, and the Y-axis, where their motion would alternate, but have very similar trajectories. That is precisely what our model has detected, where 72% of the trials had their orange angles, excluding the data for the thumb and the rotations about the Z-axis, occur in the negative elevation. A similar conclusion can be made when looking at the red angles. This corresponds to the extension of the digits creating a certain instability in which digit forces are no longer being applied orthogonally to the objects' pins [20]. What is interesting to note is that the plots seemed to have their orange angles more frequently in the negative elevation than the red angles, suggesting that the instability began to occur when the fingers were contracting from an extended posture. A similar interpretation can be made for the azimuthal direction, where the orange angles tended to be more frequently significant in the positive direction than the red angles. From the figure, we can also clearly see the general distribution and shape of all angles that were achieved throughout the trials for each digit, and be able to compare them to one another. Additionally, the density of the unstable regions in the plots correlates with the drops and repositions detected with the threshold model.

One of the factors that was not considered in this analysis is the hand proportions that were initially measured. Since we were attempting to generalize the finger pad stability limitations, we were mainly interested in the sort of angles that lead to instability, and not the total angle workspace achieved. Although, this was in part compensated by the analysis of different sized objects. Additionally, the weights of the objects could potentially undermine the real stability when handling heavier objects that are similar in size. Point-contact grasps were the main focus of this experiment, and thus we believe that the weight would have played an insignificant role, although this may need future confirmation. A few human errors were present as well. While subjects generally understood the task required for each of the trials, the ability to rotate precisely along a single axis is nearly impossible, and many had compensatory digit motions. This was especially apparent during the two finger trial around the Y-axis. This particular trial requires the subject to perform an impossible rotation when using only two fingers. We generally observed the subjects moving their index and thumb simultaneously towards and away from the palm, essentially translating the object with minor rotation occurring as a product of the trajectory. The object was also able to rotate on its own along the axis of the two digits, producing additional discrepancies for other two digit trials. We attempted to secure the object to the best of our abilities, and when the object rotated, we would ask the subjects to rotate the object back to its original position. This was not a major setback for our analysis, since we mainly focused on the angle that the object made with the finger pads, and not the rotational workspace. Future work could also focus on the angles that account for instability under different conditions, such as manipulating objects while using a rolling contact.

V. Conclusion

Apart from loss of sensitivity that comes with age, we concluded that there are other, more mechanical reasons as to why we often drop or reposition objects; finger pad friction and finger length both limit the workspace in which we are able to maintain a stable grasp on the object. There seemed to be a general trend based on observation alone; the limiting factors during in hand manipulation are the proximal portion of the friction cone and the digit length. Friction is the limiting factor for stability when the object is angled towards the palm (negative elevation angle) and the digit length is the limiting factor when the object is angled away from the palm (positive elevation angle). This was consistent for all digits other than the thumb. We have also observed a strong instability bias towards certain angles made with the finger pads. These findings play an important role in aiding our understanding of dynamic in-hand manipulation stability as well as the limitations of our hands, and should be used as inspiration for designing robotic and prosthetic digits for dexterous manipulation.

Acknowledgment

The authors would like to thank Dr. Nicolas Rojas for his participation in and input with the experimental set up.

References

[1] A. Bicchi, "Hands for dexterous manipulation and robust grasping: a difficult road toward simplicity," *IEEE Trans. on Robotics and Automation*, vol. 16, no. 6, pp. 652–662, Dec. 2000.

[2] T. Feix, J. Romero, C. H. Ek, H. B. Schmiedmayer, and D. Kragic, "A Metric for Comparing the Anthropomorphic Motion Capability of Artificial Hands," *IEEE Trans. on Robotics*, vol. 29, no. 1, pp. 82–93, Feb. 2013.

[3] M. V. Liarokapis, P. K. Artemiadis, and K. J. Kyriakopoulos, "Quantifying Anthropomorphism of Robot Hands," *IEEE Int. Conf. on Robotics and Automation*, pp. 2041–2046, May 2013.

[4] L. Birglen and C. M. Gosselin, "Optimal Design of 2-Phalanx Underactuated Fingers," *Int. Conf. on Intelligent Manipulation and Grasping*, pp. 110-116, July 2004.

[5] G. S. Guthart and J. K. Salisbury, "The Intuitive TM Telesurgery System : Overview and Application," in *IEEE Int. Conf. on Robotics an Automation*, vol. 1, pp. 618–621, 2000.

[6] V. Hayward and O. Astley, "Performance Measures for Haptic Interfaces," in *Robotics Research,* G. Giralt and G. Hirzinger, Eds. Springer London, pp. 195–207, 1996.

[7] Y. Bekiroglu, D. Kragic, and V. Kyrki, "Learning grasp stability based on tactile data and HMMs," in 19th *Int. Symposium in Robot and Human Interactive Communication*, pp. 132–137, Sept. 2010.

[8] Y. Bekiroglu, D. Song, L. Wang, and D. Kragic, "A probabilistic framework for task-oriented grasp stability assessment," in *IEEE Int. Conf. on Robotics and Automation*, pp. 3040–3047, May 2013.

[9] H. Dang and P. K. Allen, "Learning grasp stability," *Proc. IEEE Int. Conf. on Robotics and Automation*, pp. 2392–2397, May. 2012.

[10] M. K. Burstedt, J. R. Flanagan, and R. S. Johansson, "Control of Grasp Stability in Humans Under Different Frictional Conditions During Multidigit Manipulation," *J. Neurophysiology*, vol. 82, no. 5, pp. 2393–2405, Nov. 1999.

[11] R. Flanagan, M. Burstedt, and R. Johansson, "Control of Fingertip Forces in Multidigit Manipulation," *J. Neurophysiology*, vol. 81, no. 4, pp. 1706–1717, Apr. 1999.

[12] I. M. Bullock, T. Feix, and A. M. Dollar, "Dexterous workspace of human two- and three-fingered precision manipulation," in *IEEE Haptics Symposium*, pp. 41–47, Feb. 2014.

[13] T. Feix, I. M. Bullock, Y. Gloumakov, and A. M. Dollar, "Rotational Ranges of Human Precision Manipulation When Grasping Objects With Two to Five Digits," *IEEE Int. Conf. Engineering in Medicine and Biology Society*, pp. 5785-5790, Aug. 2015.

[14] I. M. Bullock, T. Feix, and A. M. Dollar, "Analyzing Human Fingertip Usage in Dexterous Precision Manipulation: Implications for Robotic Finger Design," *IEEE/RSJ Int. Conf. on Intelligent Robots and Systems*, pp. 1622–1628, Sept. 2014.

[15] P. Cesari and K. M. Newell, "Body-scaled transitions in human grip configurations," *J. Exp. Psychol. Human Perception and Performance*, vol. 26, no. 5, pp. 1657–1668, Oct. 2000.

[16] P. Cesari and K. M. Newell, "The scaling of human grip configurations," *J. Exp. Psychol. Human Perception and Performance*, vol. 25, no. 4, pp. 927–935, Aug. 1999.

[17] R. Glister, C. Hesse, and H. Deubel, "Contact points during multidigit grasping of geometric objects," *Exp. Brain Res.*, vol. 217, no. 1, pp. 137-151, Mar. 2012.

[18] N. I. Fisher, T. Lewis, and B. J. J. Embleton, "Statistical analysis of spherical data," 1st ed. Cambridge, Great Britain: Cambridge University Press, 1987.

[19] P. Leong and S. Carlile, "Methods for spherical data analysis and visualization," *J. of Neuroscience Methods*, vol. 80, no. 2, pp. 191–200, Apr. 1998.

[20] J.B.J. Smeets and E. Brenner, "A New View on Grasping," *Motor Control*, vol. 3, pp. 237–271, July 1999.